Supporting Information

Seed-Mediated Growth of Ultra-Thin Triangular Magnetite Nanoplates

Zheheng Xu, Zengyan Wei, Peigang He, Xiaoming Duan, Zhihua Yang, Yu Zhou and Dechang Jia*

Department of Materials Science and Institute for Advanced Ceramics, School of Material Science and Engineering, Harbin Institute of Technology, Harbin 150001, P. R. China

1. Chemicals and Materials. Oleic acid (OA, 95%), iron(III) chloride hexahydrate ($FeCl_3 \cdot 6H_2O$, 98%), sodium oleate (95%), hexane (AR), ethanol (AR), toluene (AR) and diethylene glycol (AR) were purchased from Sinopharm Reagents. 1-octadecene (ODE, 90%), *N*-hydroxysuccinimide (NHS, 98%), 1-Ethyl-3-[3-dimethylaminopropyl]carbodiimide (EDC, 98.0%), poly(acrylic acid) (M_w 2000) and monofunctional amine-terminated poly(ethylene glycol) (MW 5000) were supplied by Aladdin Reagents. All the chemicals and materials were used as received without further purification.

2. Synthesis of Iron(III) Oleate Complex. Iron(III) oleate (FeOL) was prepared by the method adapted from Park *et al.* [ref. 35]. Briefly, 10.8 g of $FeCl_3 \cdot 6H_2O$, 36.5 g of sodium oleate, 80 mL of ethanol, 60 mL of deionized water, and 140 mL of hexane were mixed and refluxed for 4 h. Next, the mixture was transferred to a separatory funnel. The organic layer containing FeOL was

separated and purified by washing with 30 mL of deionized water three times. The waxy brown-colored product was collected after removing the solvent by rotary evaporation, and was stored at 4°C before use.

3. Preparation of ultra-thin nanoplates of Fe_3O_4. In a typical synthesis of triangular nanoplates, 1 mmol of FeOL and 5 mL of ODE were mixed and heated to 120ºC. The solution was kept at this temperature for 20 min under a flow of nitrogen, and the resulting solution was named as solution A. Next, seeds were formed by heating solution A at 310°C for 1 min. Meanwhile, 2 mmol of OA was dissolved in another 5 mL of solution A, and the resulting solution was rapidly injected into the reaction flask containing seeds. The reaction temperature suddenly decreased to 240°C, and the growth reaction was allowed to proceed for 1 h at this temperature. The product was purified using the solvent/non-solvent pair of hexane/ethanol three times.

4. The ligand-exchange process for the phase transfer. 0.5 g of poly(acrylic acid) (M_w∼2000) was dissolved in 8 mL diethylene glycol and heated to 110°C under nitrogen for 30 min. The solution was then heated to 240°C, followed by injecting 1 mL of triangular Fe_3O_4 nanoplates dispersed in toluene (∼50 mg/mL) under stirring. After heating the mixture for 5 min at 240°C, poly(acrylic acid)-coated Fe_3O_4 nanoplates were separated with centrifugation, and washed with ethanol once and with water three times. Next, 10 mg of poly(acrylic acid)-coated Fe_3O_4 nanoplates was dispersed in 10 mL of water, and activated with NHS/EDC for 30 minutes (20 mM NHS, 20 mM EDC). Then, 50 mg of monofunctional amine-terminated poly(ethylene glycol) (MW 5000) was added. The solution was stirred at room temperature overnight. The nanoplates coated with poly(ethylene glycol)-*g*-poly(acrylic acid) were collected by centrifugation and washed with water three times.

5. Characterization and Measurements. TEM and SAED images were captured on a JEM2100 (JEOL) transmission electron microscope with an accelerating voltage at 200 kV. Samples were prepared by drying 10 μL of the Fe_3O_4 nanoplate in hexane on carbon-coated copper grids. HRTEM imaging were performed on a Tecnai G2 F30 (FEI) microscope operated at 300 kV. XRD

measurements were carried out on a Rigaku Ultimate-IV X-ray diffractometer operating at 40 kV/30 mA using Cu Kα line (λ = 1.5418 Å). XPS measurements were performed on an ESCALAB 250Xi X-ray photoelectron spectrometer (Thermo Fisher Scientific). The binding energy of all analyses was calibrated using the C 1s peak at 284.6 eV. FTIR spectra were recorded on a Perkin-Elmer Spectrum One Spectrophotometer. AFM was measured on a stand-alone Bruker Dimension Icon atomic force microscope with a typical probe tip radius of 10 nm. All images were taken in the contact mode, and treated with the WSxM software to enhance the imaging contrast [ref. 28]. Inductively coupled plasma optical emission spectrometry (ICP-OES) was used to quantify the content of metal, which was conducted on a SPECTRO GENESIS ICP spectrometer. The magnetic properties of the samples were recorded on a vibrating sample magnetometer (VSM 7404, Lakeshore) in magnetic field range of 10 kOe at 300 K. The phantom study of MRI was performed on a 3 T Prisma MR scanner (Siemens Healthcare). Samples was prepared with Fe concentrations, [Fe], ranges of 800, 400, 200, 100, and 50 μM, and with water at 0 μM for comparison. T_2-weighted and T_1-weighted MR images were collected under the following parameters: TR/TE = 2000/80 ms (T_2), TR/TE = 300/10 ms (T_1).

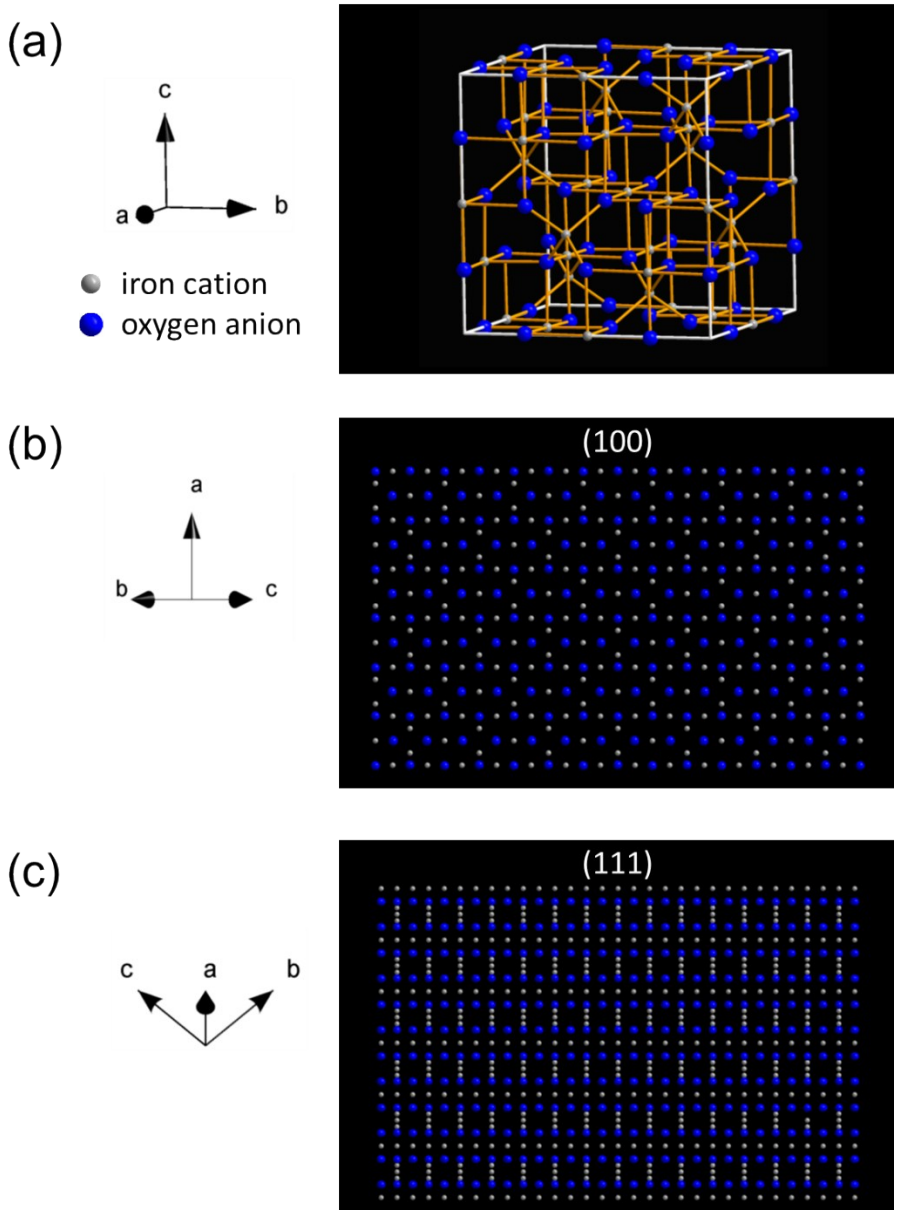

Fig. S1. (a) Crystal structure of Fe_3O_4. (b) Side view of the (100) facet of Fe_3O_4. (c) Side view of the (111) facet of Fe_3O_4.

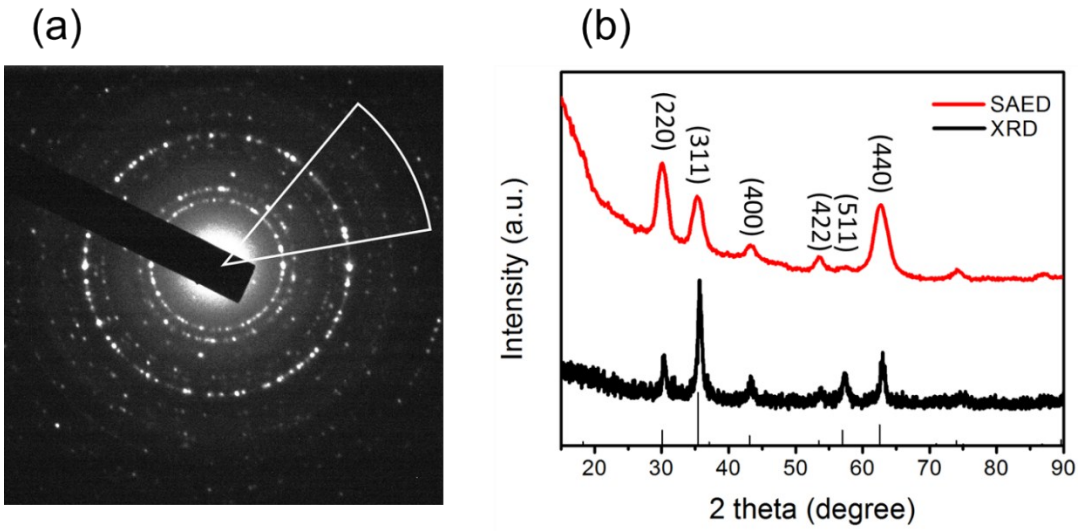

Fig. S2. (a) SAED image of triangular Fe_3O_4 nanoplates. The integration area in the radial profile analysis is highlighted with a white sector. (b) Integrated SAED and XRD patterns of triangular Fe_3O_4 nanoplates. The standard XRD patterns for Fe_3O_4 (PDF No. 65-3107) are listed at the bottom.

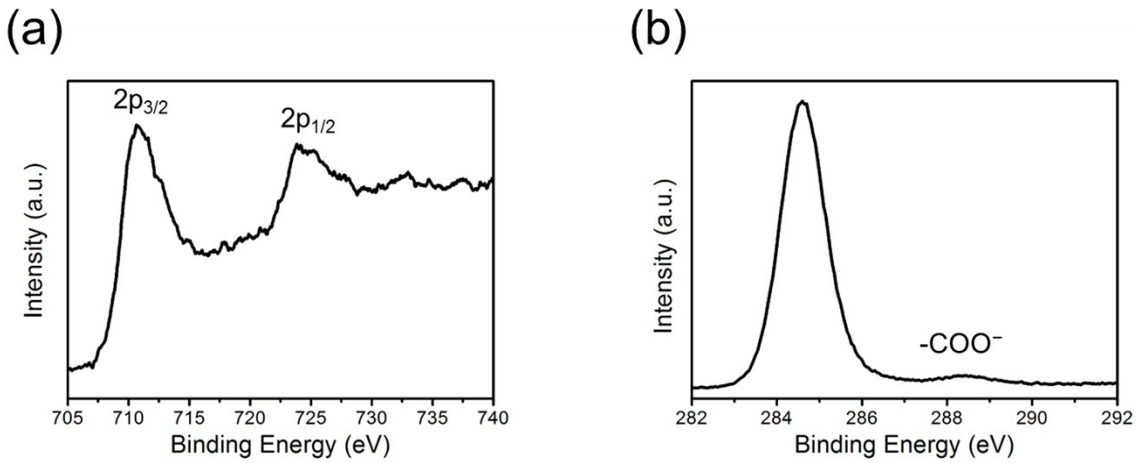

Fig. S3. XPS spectra of triangular Fe_3O_4 nanoplates. (a) Fe 2p spectra and (b) C 1s spectra.

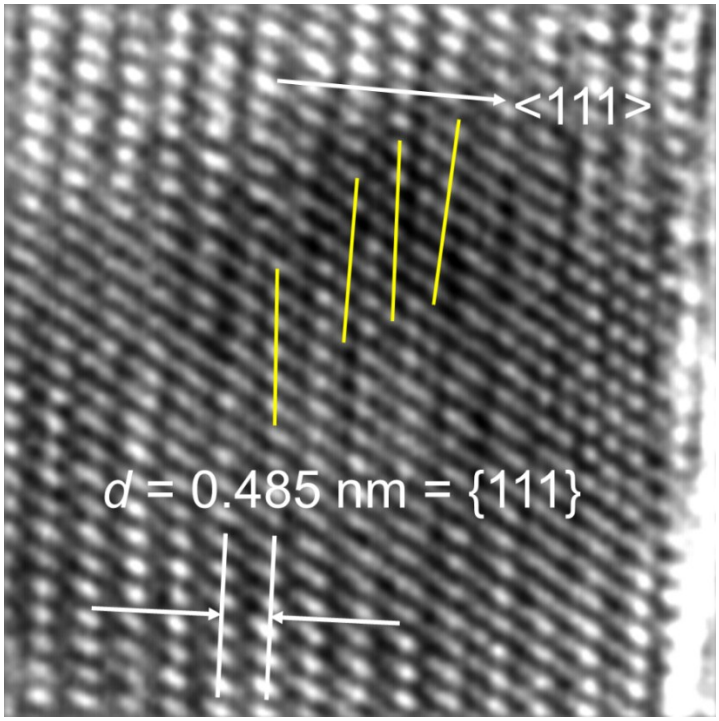

Fig. S4. An inverse FFT image corresponding to the highlighted area in Fig. 3b. Edge dislocations are highlighted with yellow lines.

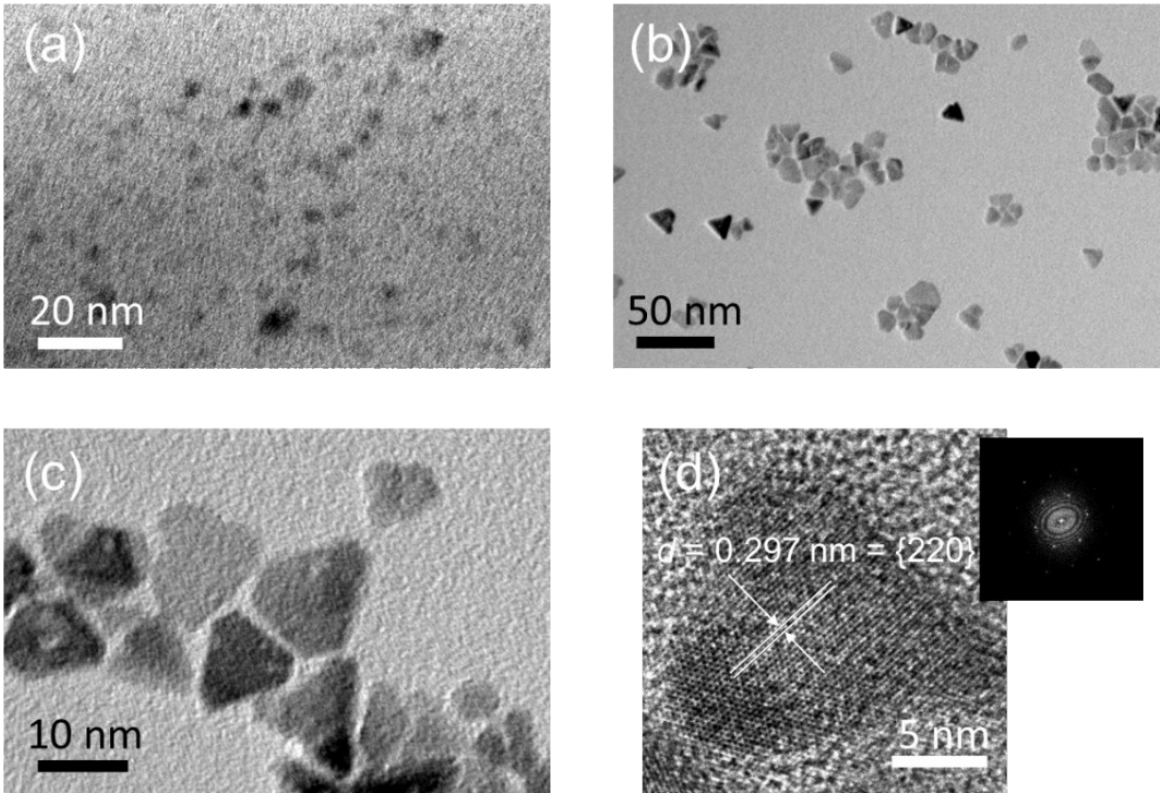

Fig. S5. (a) TEM image of Fe_3O_4 nanoparticles prepared after 1 min incubation at 310ºC. (b) Low- and (c) high-magnification TEM images of truncated triangular Fe_3O_4 nanoplates prepared under the same condition as in Fig. 1 except that the incubation time was shortened to 30 min at 240ºC. (d) HRTEM image with the corresponding FFT patterns of truncated triangular Fe_3O_4 nanoplates in (c).

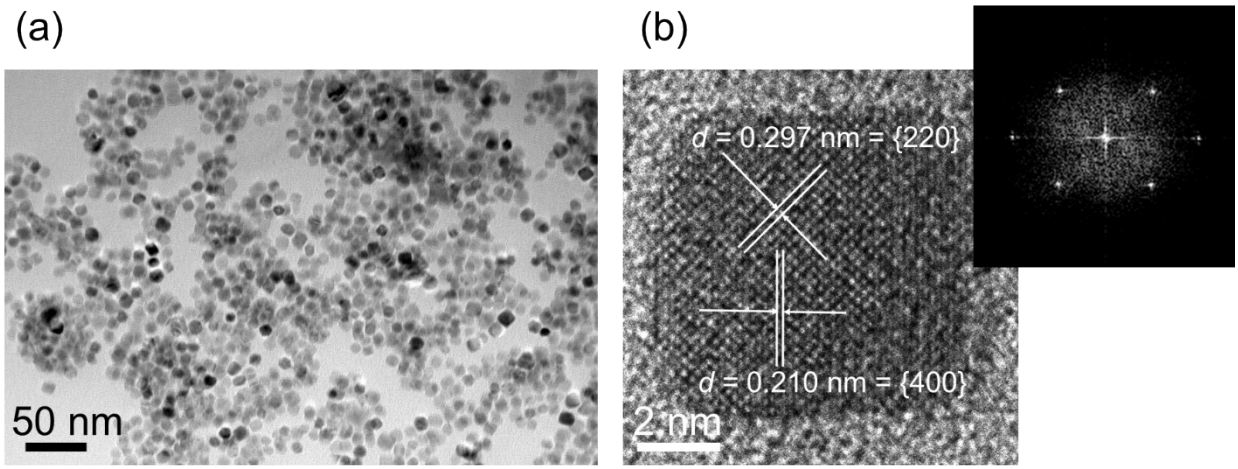

Fig. S6. (a) TEM and (b) HRTEM images with the corresponding FFT patterns of Fe_3O_4 nanoparticles after prolonging the nucleation period to 5 min at 310ºC.

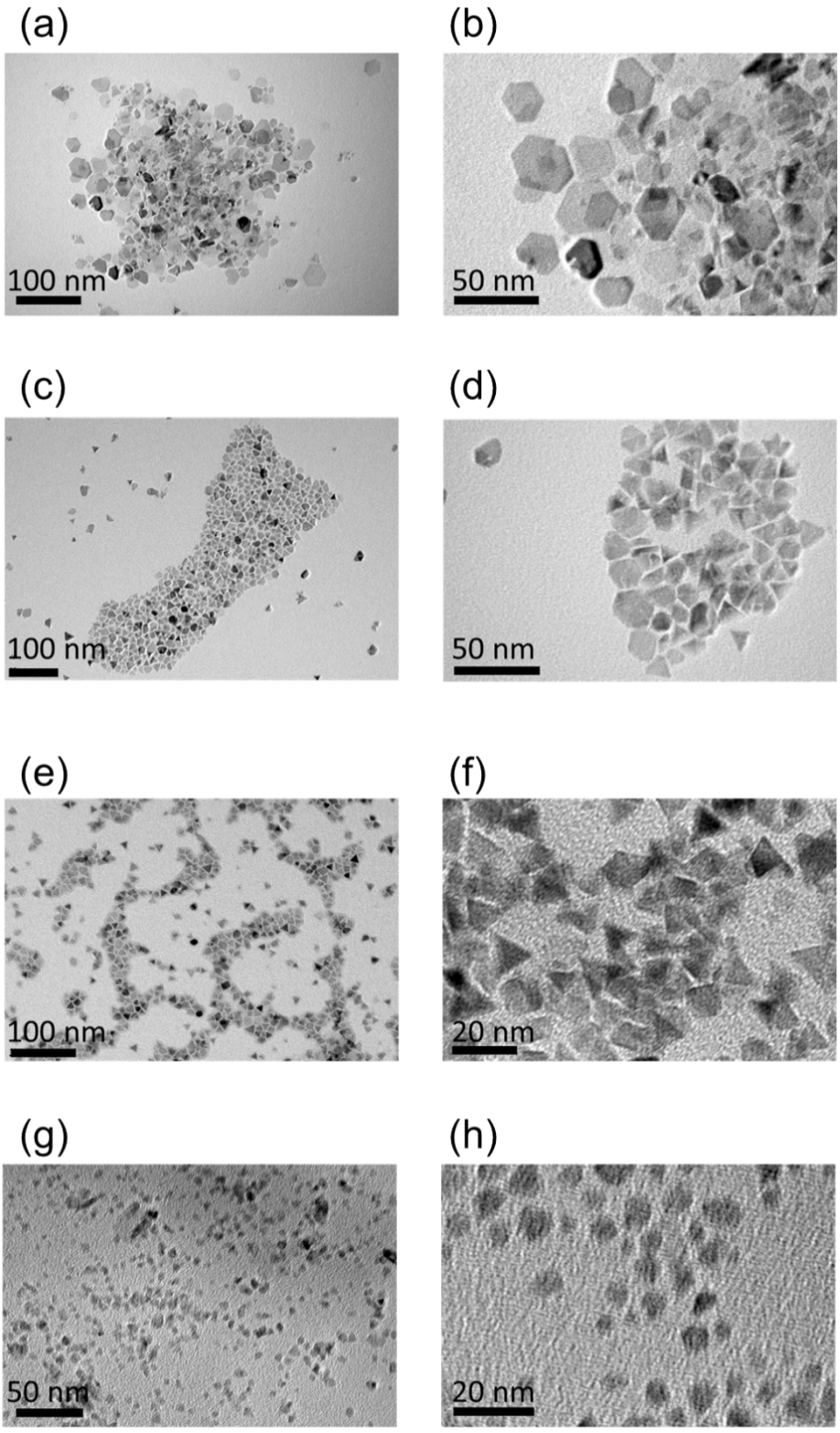

Fig. S7. TEM images showing the variation in morphology for samples prepared by changing the amount of OA while keeping other conditions the same as in Fig. 1. (a, b) No OA; (c, d) 1 mmol OA; (e, f) 2.5 mmol OA; (g, h) 3 mmol OA.

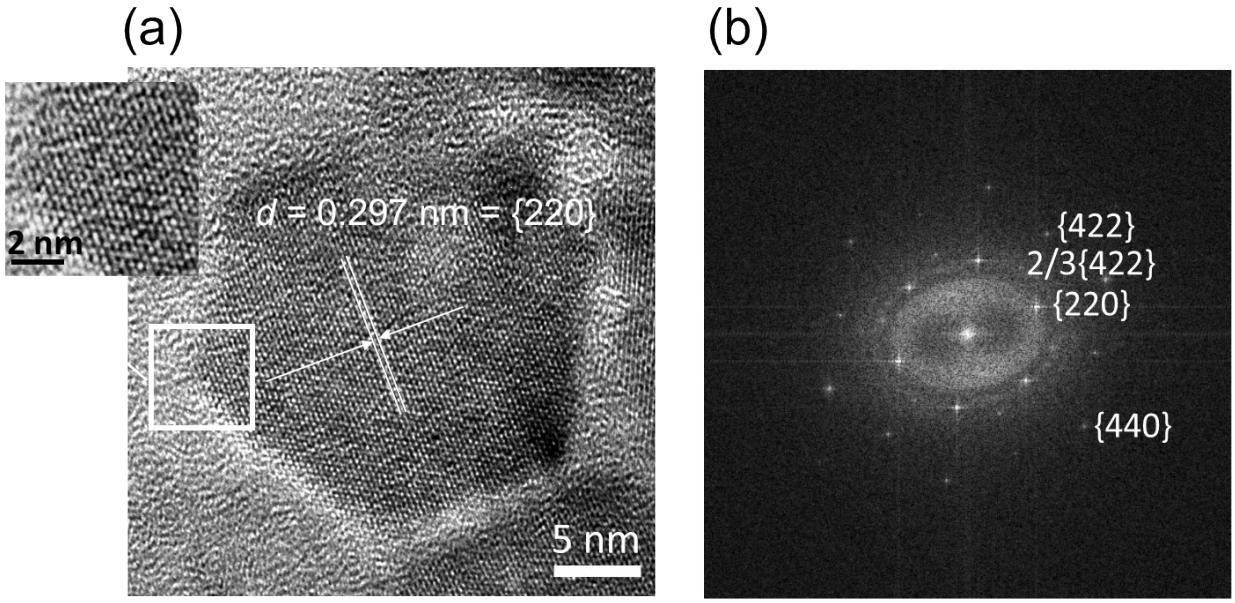

Fig. S8. (a) HRTEM images and (b) the corresponding FFT patterns of the hexagonal Fe_3O_4 nanolate. Inset in (a) gives a magnified image of the square area highlighted in (a). In (b), {220} reflections show a 6-fold symmetry. In addition, 2/3{422} forbidden reflections are observed. All of these indicate that, similar to triangular nanoplates, the flat surfaces on the top and bottom of the hexagonal nanoplate are bound by {111} [ref. 10, 21-27].

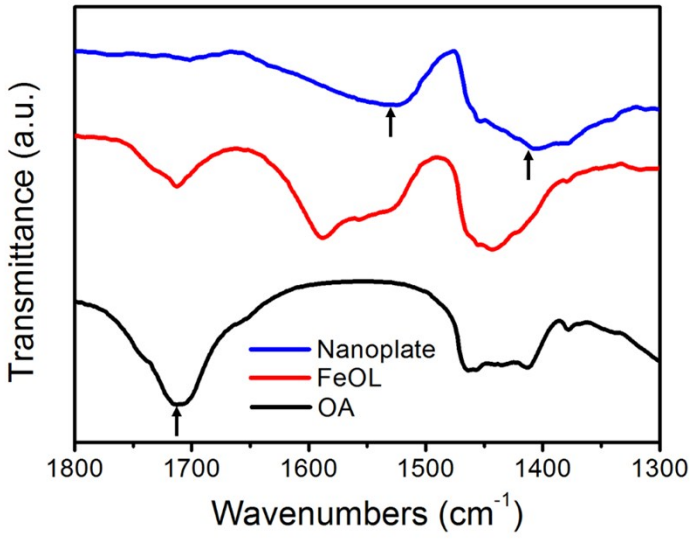

Fig. S9. FTIR spectra of triangular Fe_3O_4 nanoplates prepared in the presence of OA, FeOL and OA, respectively.

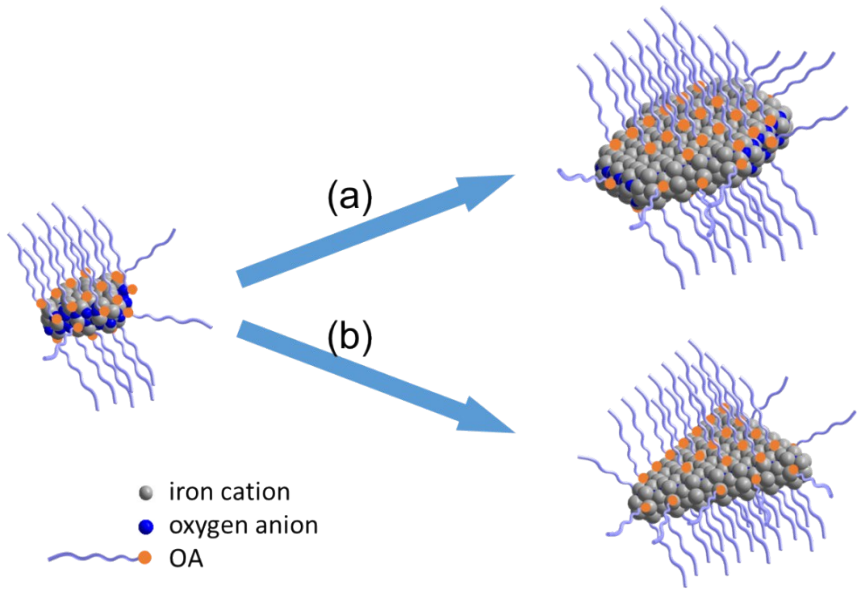

Fig. S10. Scheme illustrating the influence of OA on the shape evolution of Fe_3O_4 nanoplates. (a) Hexagonal nanoplates were prepared without an extra addition of OA; and (b) triangular nanoplates were prepared after adding 2~2.5 mmol OA. Analogous to fcc lattice, the side surfaces of a Fe_3O_4 hexagonal nanoplate could be bound by a mix of {111} and {100} planes [ref. 22, 25]. Without adding OA, oleic ion formed by the decomposition of FeOL was mainly adsorbed on the flat surfaces on the top and bottom of Fe_3O_4 nanoplates, and both {100} and {111} side surfaces were less protected, probably due to the presence of a large amount of less protected atoms located on edges. Therefore, hexagonal nanoplates were prepared (Fig. S10a). The extra addition of OA can passivate {111} side facets. Consequently, shape transformation from hexagonal nanoplates to triangular nanoplates enclosed by {111} alone was observed by increasing the amount of OA (Fig. S10b). When an extreme amount of OA was added, all facets of seeds were adsorbed by OA, and the growth was strongly impeded, leading to nanoparticles having similar morphology to seeds.

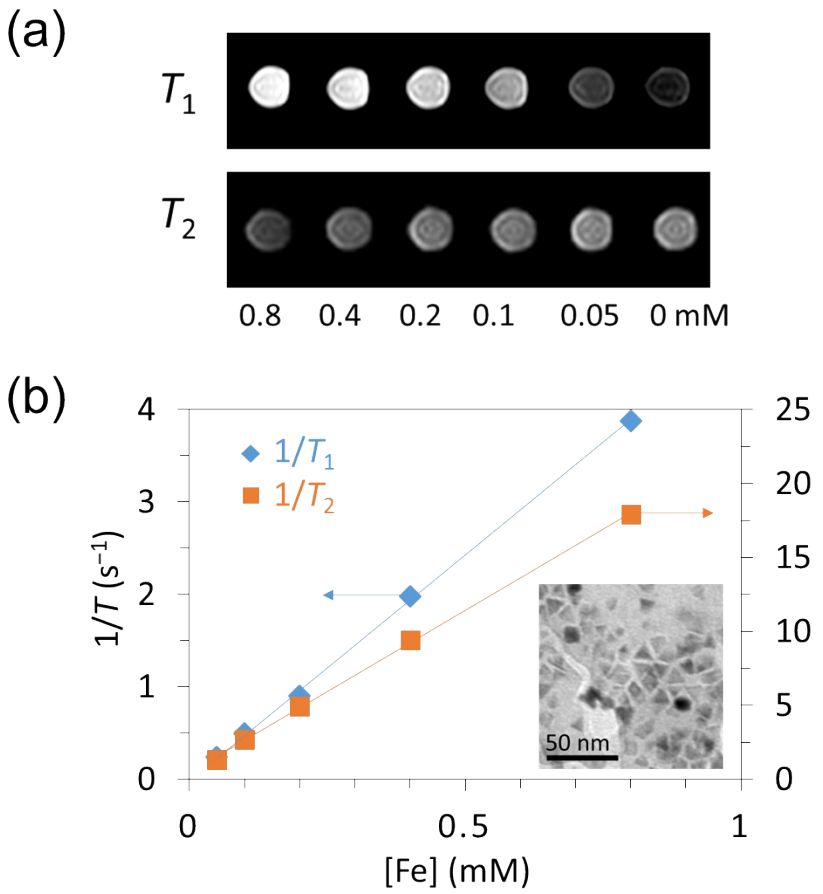

Fig. S11. (a) T_1- and T_2-weighted phantom imaging of triangular Fe_3O_4 nanoplates. (b) Relaxivity measurements of triangular Fe_3O_4 nanoplates at 3 T. The specific relaxivity r_1 and r_2 are indicated by the slopes, which are 4.87, and 21.92 $mM^{-1}{\cdot}s^{-1}$, respectively. Inset: TEM image of triangular Fe_3O_4 nanoplates coated with poly(ethylene glycol)-*g*-poly(acrylic acid) after the ligand exchange.